Long-Short Rupture Boundary of Coseismic Displacement Estimation Based on 30-Seconds GNSS Observation

Rizki, A. A.[1] | Pratama, C.[2] ✉ | Heliani, L. S.[3] | Wibowo, A.[4] | Sahara, D. P.[5]

1. Department of Geodetic Engineering, Faculty of Engineering, University Gadjah Mada, Yogyakarta, Indonesia. E-mail: agan.aul.rizki@mail.ugm.ac.id

2. **Corresponding Author**, Department of Geodetic Engineering, Faculty of Engineering, University Gadjah Mada, Yogyakarta, Indonesia. E-mail: cecep.pratama@ugm.ac.id

3 Department of Geodetic Engineering, Faculty of Engineering, University Gadjah Mada, Yogyakarta, Indonesia. E-mail: lheliani@ugm.ac.id

4. Department of Informatics, Faculty of Science and Mathematics, Diponegoro University, Semarang, Indonesia. E-mail: bowo.adi@live.undip.ac.id

5. Global Geophysics Research Group, Institut Teknologi Bandung, Bandung, Indonesia. E-mail: david.sahara@gf.itb.ac.id

Abstract

Indonesia is located at the Pacific Ring of Fire and the meeting place of the world's four tectonic plates, which makes Indonesia to have a high tectonic activity and to be prone to earthquakes. Currently, early earthquake detection service in Indonesia is based on seismometers network. However, seismometer instruments that observe seismic waveforms might become saturated, and as such may lead to incorrect earthquake magnitude detection at an early stage. Therefore, a new approach is needed to detect earthquake coseismic information. Global Navigation Satellite System (GNSS) is a good instrument to measure the surface displacement due to an earthquake. However, previous studies in Indonesia still predominantly used daily solution data. To carry out early detection, it is not possible to use daily solutions. Therefore it is needed to use the data with a higher frequency solution than the daily solution. In this study, we used 30-second sampling rate data available from Indonesian Continuously Operating Reference Station (Ina-CORS) and Sumatran GPS Array (SuGAr). We will see how the 30-second GNSS data responds to earthquakes to estimate the value of coseismic displacement compared to daily solution data. The estimated value of this coseismic displacement can be used for earthquake early detection.

Keywords: Earthquake, Kinematic, Duration, Geodetic, Tectonic.

1. Introduction

Indonesia, being located in the Pacific Ring of Fire and in the meeting place of four of the world's tectonic plates makes it to have high tectonic activity. This high tectonic activity makes Indonesia being prone to earthquakes (Pusat Studi Gempa Nasional, 2017). Earthquakes have a repeating phase called an earthquake cycle. The phase during the main earthquake when the vibrations are felt the strongest and there is a sudden displacement in the crust is called the coseismic phase. Some of the earth's crust may undergo displacement both vertically and horizontally during the coseismic phase of an earthquake (Sarsito et al., 2005).

Coseismic information on earthquakes that occur can be detected using seismometer data recorded using inertial sensors. However, seismometer data is not able to predict the development of the magnitude of an earthquake quickly (Ruhl et al., 2017). Therefore, a new approach is needed to detect earthquake coseismic information. Previous research has stated that the Global Navigation Satellite System (GNSS) is a good instrument for measuring ground displacement around earthquakes (Kawamoto et al., 2017; Larson, 2009). It has developed into a multidisciplinary field of GNSS seismology. GNSS seismology uses a geodetic approach to analyze GNSS data at a high sampling rate. In addition, other studies suggest that 30-second GNSS can be used to complement seismic approaches using seismometers (Ruhl et al., 2017). Therefore, it is necessary to conduct research to see the

ability of GNSS with a high sampling rate to be able to record ground displacements due to the earthquake rupture activity in the coseismic phase.

Research conducted by Pratama et al. (2018) with a study on the 2012 Indian Ocean earthquake showed that the earthquake activity could be recorded using daily solution of GNSS data. Thus, it could evaluate the magnitude of the coseismic offset both in horizontal and vertical components. This GNSS data information is then used to evaluate the most suitable coseismic model for the case of earthquake (Pratama et al., 2018). However, the study has not compared the daily displacement solution with the shorter solution time after the earthquake with the 30-second data available in Ina-CORS (Pratama et al., 2019; Susilo et al., 2017) and SuGAr (Feng et al., 2015). Therefore, this study was conducted to determine the coseismic displacement of earthquakes from the 30-second solution GNSS data and compared it with the daily solution.

2. Data and Methods
2-1. Earthquake Data
The earthquake data used is the data about five earthquakes occurred in Indonesia and shown in Figure 1. The five earthquakes include the 2012 Indian Ocean earthquakes (Mw 8.6 and Mw 8.2), the 2018 Lombok earthquake (Mw 6.9), the 2017 Kampungbaru earthquake (Mw 6.5), and the 2019 Simpang earthquake (Mw 4.9). All the earthquake data are derived from Indonesian Meteorology, Climatology and Geophysics Agency (BMKG) catalog data.

2-2. 30-second Solution and Daily Solution of GNSS Data
We obtained all permanent GNSS stations in Java, Sumatra and Lombok. The focus of this study is to determine whether the results of the displacement values of the two conditions are significantly different or not. The first condition is the position of the 30-second solution before and after the earthquake with

data in the form of file observations of stations located around the earthquake. The names of these stations are SAMP, BSIM, LEWK, CMAT, CRUT, CPMK and CMIS. All the stations are shown in Figure 1, with the day of observation when the earthquake took place. The binding point files used are observation files for NTUS and BAKO stations. This observation file has a *.yyo format that comes from the Indonesian Geospatial Information Agency (BIG). The supporting data needed are precise ephemeris data (.sp3) and ionospheric data.

The processing 30-second data coordinates them using the differential method of GAMIT Track Kinematic (Herring et al., 2015) (Figure 2). Track processing looks for phase ambiguity to improve the pseudo-ranges from the GNSS data so that the distance value obtained becomes more accurate to obtain the final coordinate value of the processing (Huang et al., 2017).

The second condition is the daily position of the same station with a range of data, five days before and after the earthquake. These data are used as a comparison of the first condition. Those GNSS stations are included in the Indonesian Continuous Operating Reference Stations (Ina-CORS) network operated by the Geospatial Information Agency of Indonesia. We estimated positions based on daily GNSS coordinate time series.

2-3. Earthquake Rupture Duration
Earthquake rupture duration is the time of earthquake to take rupture proceed along a fault. Determination of the duration of the earthquake rupture is needed to estimate the earthquake coseismic displacement. This is because the displacement is the difference between the position before and after the earthquake rupture. The approximate duration of the earthquake is obtained by adding up the time that the earthquake is felt from the BMKG's catalog and the duration of the earthquake rupture. The earthquake rupture duration is consisting of the start time and the end time of the earthquake.

(a)

(b)

(c)

(d)
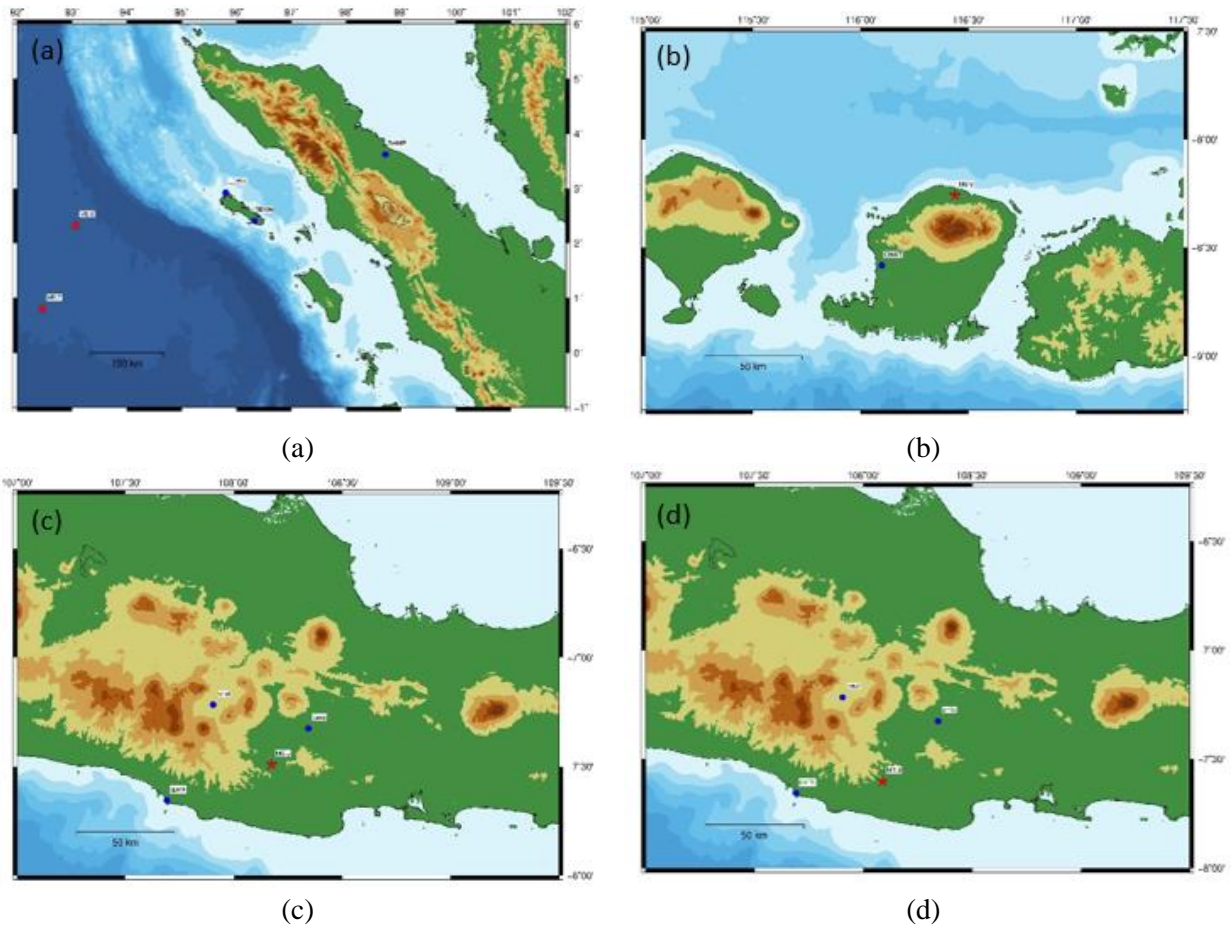
Figure 1. Location of the GNSS station (blue) and the epicenter (red) of the Sumatran Indian Ocean Mw 8.6 and Mw 8.2 (a), Lombok Mw 6.9 (b), Kampungbaru, Java Mw 6.5 (c) and Simpang, Java earthquake Mw 4.9 (d).
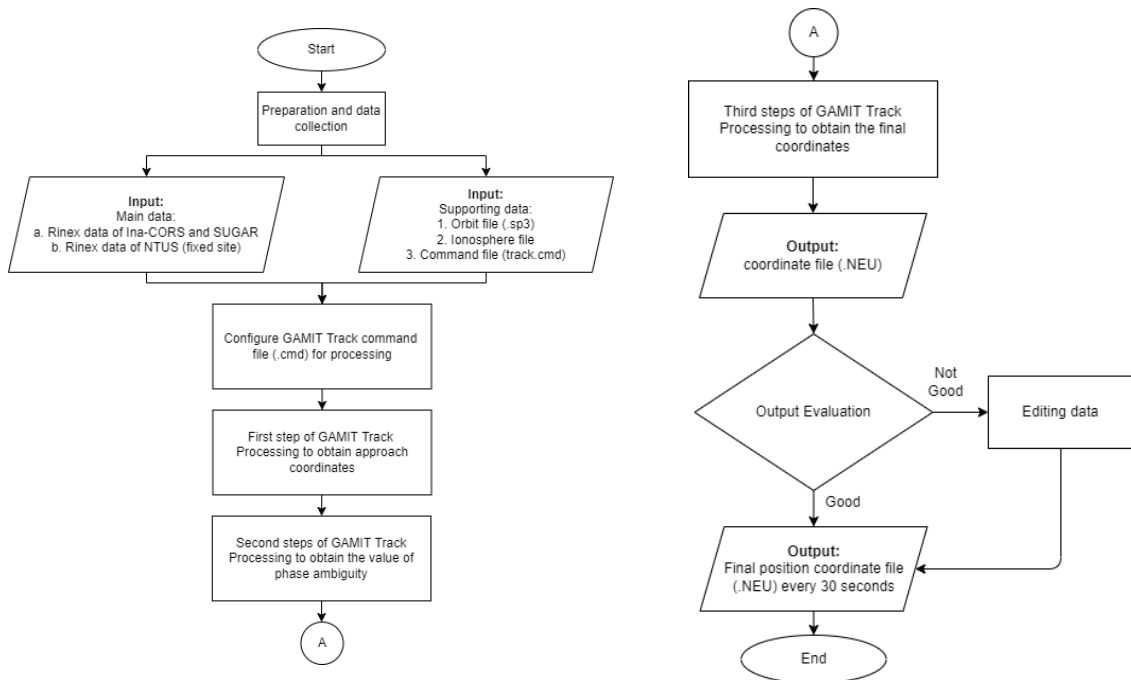
Figure 2. 30-Second Kinematic GNSS processing flowchart using GAMIT Track.

The duration of the rupture is obtained from previous research literature studies for Indian Ocean (Wei et al., 2013) and Lombok (Priadi et al., 2020) earthquakes. Meanwhile, the other obtained the duration using earthquake scaling (Wells & Coppersmith, 1994). The calculation of the duration of the earthquake rupture is estimated using a multiplication approach between the length and the velocity of the rupture. The length of the rupture is estimated using the earthquake scaling laws approach. It is obtained from an empirical correlation with the earthquake magnitude (Wells & Coppersmith, 1994; Blaser et al., 2010). Then for the rupture velocity using the median value of the average earthquake rupture velocity obtained as 2850 m/s (Chounet et al., 2018).

2-4. Coseismic Displacement
In this study, the used data are 30-second rate kinematic positions computed by using GAMIT Track Kinematic. Then, the daily position data is obtained from the Indonesian Geospatial Information Agency (BIG). For 30-second data, the taken time spans are the positions at one minute before and after the earthquake rupture. For the daily solution, the taken time span is five days before and after the earthquake. In this way, the position before and after the earthquake rupture are obtained within the time span along with the corresponding standard deviations.

The calculation of the coseismic displacement (d) is done by differentiating the coordinates of the position before (epoch I) and after (epoch II) of the earthquake rupture due to the coseismic phase (1). The positions before and after the earthquake rupture are averaged according to the range of data used so that the average position before the rupture (r_1) and the average position after the rupture (r_2) is obtained. The calculation of the standard deviation of the displacement value is obtained by random error propagation with the standard deviation of positions data before (r_1) and after (r_2) earthquake rupture in coseismic phases (2) and (3).

$$d = r_2 - r_1 \tag{1}$$

$$\Sigma_d = G\Sigma_{r_2 r_1} G^T \tag{2}$$

$$S_d^2 = \left(\frac{\partial d}{\partial r_2} \frac{\partial d}{\partial r_1}\right) \begin{pmatrix} S_{r_2}^2 & 0 \\ 0 & S_{r_1}^2 \end{pmatrix} G^T \tag{3}$$

Displacement variant (S_d^2) is calculated using error propagation (2) and (3), where, Σ_d is the displacement covariance matrix calculated using error propagation matrix (G). The covariance matrix of the second and the first epoch is $\Sigma_{r_2 r_1}$. Position variants after rupture due to the coseismic phase epoch I and II are $S_{r_1}^2$, $S_{r_2}^2$.

Next, to find out whether the displacement of a point is significant or not, a statistical test is carried out with t-student distribution with 95% confidence level and infinite degrees of freedom ($t_{(\alpha/2,r)}$). Statistical tests are also used to find out whether the displacement of two solutions in the 30-second (d_1) and daily solution (d_2) are significantly different or not.

This analysis was conducted to test whether displacement of a point is significant or not by comparing the value of t between two parameters (4) and the value of t-student distribution variable ($t_{(\alpha/2,r)}$) with 95% confidence level and infinite degrees of freedom (5).

$$t = \left| \frac{(d_1 - d_2)}{\sqrt{\sigma d_1^2 + \sigma d_2^2}} \right| \tag{4}$$

$$t > t_{(\alpha/2,r)} \tag{5}$$

3. Result and Discussion
3-1. The Difference between Coseismic Displacement Values of 30-second Solution and Daily Solution
The calculation of the coseismic displacement (d) is done by differentiating the coordinates of the position before (epoch I) and after (epoch II) the earthquake rupture due to the coseismic phase. The following time series data from 30-second solution is shown in Figure 3, and the displacement data resulted from 30-second kinematic and daily solution data are shown in Table 1.

Then, the value of the displacement difference is estimated by calculating the difference value of the displacement in the five-day daily solution with the 30-second solution within a minute before and after the earthquake. Especially, for the Indian Ocean

earthquake, since there are two earthquakes in one day, the 30-second solution displacement data of the Indian Ocean (Mw 8.6 and Mw 8.2) are added together to compare with the daily solution displacement data. The following data is resulted from the calculation of the difference in the value of the displacement in the processing of the 30-second kinematic solution with a time span of one minute with the value of the daily solution displacement. This is from an earthquake with the standard deviation of the displacement difference calculated using error propagation shown in Table 2.

(a)

(b)

(c)

(d)

(e)
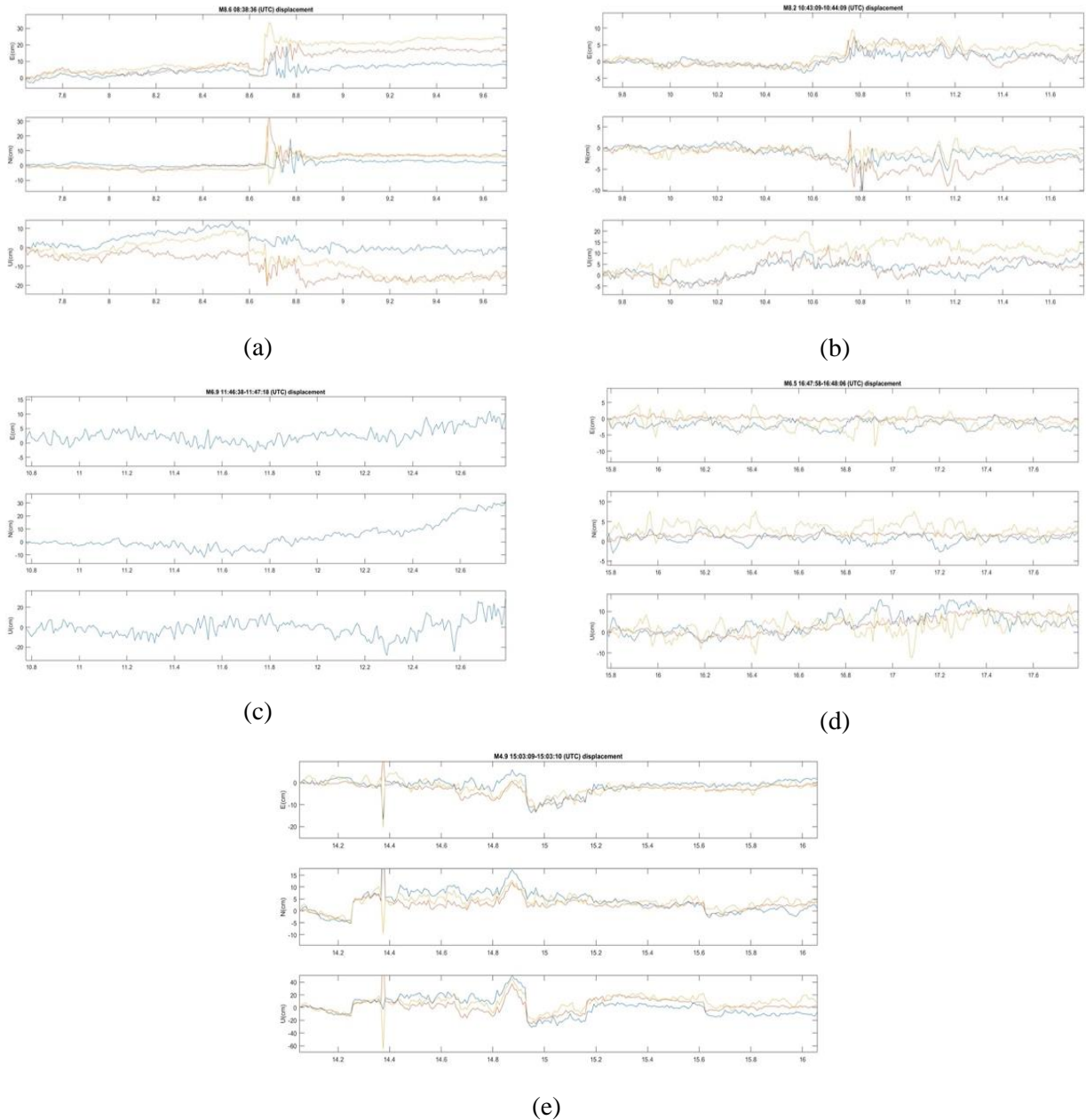
Figure 3. Time series of 30-second kinematic solutions for (a) Mw 8.6 Indian Ocean Earthquake, (b) Mw 8.2 Indian Ocean Earthquake, (c) Mw 6.9 Lombok Earthquake, (d) Mw 6.5 Kampungbaru Earthquake and (e) Mw 4.9 Simpang Earthquake. Each color represents each GNSS station.

Table 1. Displacement value of 30-second kinematic with one-minute time span before and after the rupture, and displacement value of daily solution with the time span of five days before and after the rupture.

Earthquake & GNSS Station	Coseismic Displacement Value (cm)					
	30-Second Kinematic Solution			Daily Solution		
	dN	dE	dU	dN	dE	dU
Indian Ocean Mw 8.6 SAMP	-1.855	13.38	-3.53	2.685	7.2948	-1.6116
Indian Ocean Mw 8.2 SAMP	-1.26	1.5	-0.84			
Indian Ocean Mw 8.6 BSIM	14.215	7.525	1.69	6.56572	17.78684	-2.23812
Indian Ocean Mw 8.2 BSIM	-1.165	3.85	-0.755			
Indian Ocean Mw 8.6 LEWK	-5.68	28.585	-2.545	11.33516	25.90362	-4.41752
Indian Ocean Mw 8.2 LEWK	0.695	1.405	1.265			
Lombok Mw 6.9 CMAT	6.83	1.175	3.06	6.896	1.9714	-1.68
Kampungbaru Mw 6.5 CMIS	-0.19	2.19	-4.24	-0.259	0.2264	-0.465
Kampungbaru Mw 6.5 CPMK	0.075	0.165	-1.53	-0.179	0.1999	-0.17
Kampungbaru Mw 6.5 CRUT	-0.28	-2.07	1.045	-0.08	0.4136	0.0288
Simpang Mw 4.9 CMIS	-0.08	-0.83	1.915	0.1462	0.1486	-0.936
Simpang Mw 4.9 CPMK	0.26	0.38	2.325	-0.011	-0.045	-0.356
Simpang Mw 4.9 CRUT	-0.37	1.325	7.59	-0.141	-0.015	0.8705

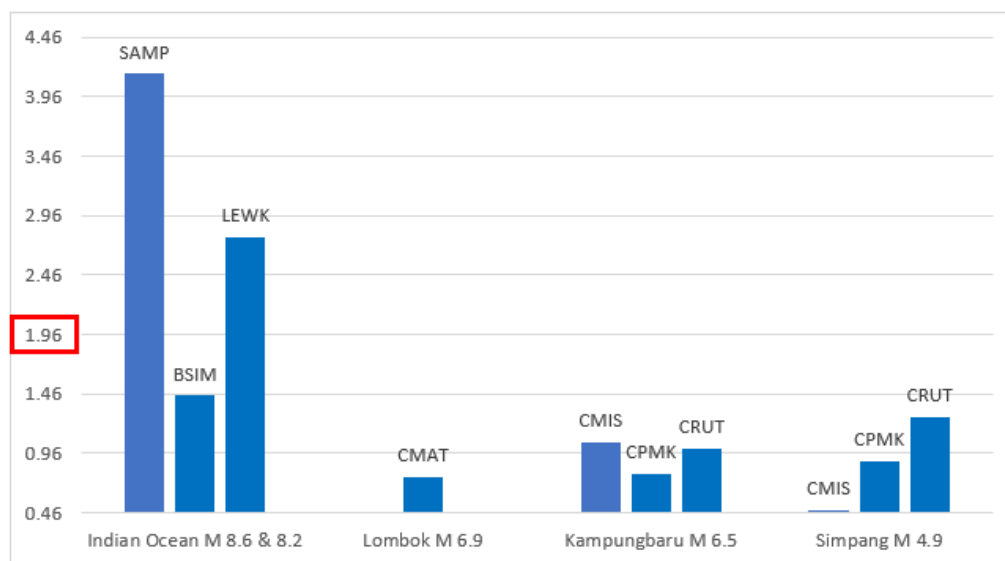**Table 2.** The difference displacement value of 30-second kinematic solution with daily solution.

Earthquake/Site	The Difference Displacement Value (cm)			
	ΔdN	ΔdE	ΔdU	$\Delta d3D$
Indian Ocean SAMP	5.8	-7.58	2.75	9.94
Indian Ocean BSIM	-6.48	6.41	-3.17	9.65
Indian Ocean LEWK	16.32	-4.09	-3.14	17.11
Lombok CMAT	0.07	0.80	-4.74	4.81
Kampungbaru CMIS	-0.07	-1.96	3.78	4.26
Kampungbaru CPMK	-0.25	0.03	1.36	1.38
Kampungbaru CRUT	0.19	2.48	-1.02	2.69
Simpang CMIS	0.23	0.98	-2.85	3.02
Simpang CPMK	-0.27	-0.43	-2.68	2.73
Simpang CRUT	0.23	-1.34	-6.72	6.86

From the data in Table 2, it can be seen that the value of the displacement difference varies. The biggest difference value is seen in the case of the Indian Ocean earthquake, especially the LEWK station, which reaches 17 cm. In the case of other earthquakes, the value of the displacement difference has a smaller value than the Indian Ocean earthquake, ranging from 1 to 6 cm.

3-2. Statistical Test of Two Parameter Differences.

Statistical tests were conducted to determine whether the two values were significantly different or not. The two displacement values from the 30-second solution were tested against the daily solution using a two-parameter statistical difference test. The null hypothesis (Ho) is that the two parameters are significantly different, with the alternative hypothesis of not being significantly different. Ho is accepted on the condition that the t value is greater than the t-table value (1.96) so that the two parameters are significantly different. However, if the value of t count < t table, then the two parameters are not significantly different. The result of the statistical test is shown in Figure 4.

Figure 4. The results of the statistical test for the difference between the displacements derived from 30-second kinematic solutions with daily solutions.

In Figure 4, it can be seen that those with a t value bigger than the t-table value (>1.96) are SAMP and LEWK stations in the Indian Ocean earthquake, while other stations have values less than the t-table (<1.96). Therefore, the data that has a significant difference is only at the two stations in the Indian Ocean earthquake. Meanwhile, in the other three earthquake cases, the displacement value is not significantly different between the 30-second solution and the daily solution.

In Figure 5a, it can be seen that the difference in the displacement value is quite clear at the three Indian Ocean earthquake stations in which the 30-second solution has a much larger displacement value. As to the horizontal direction displacement, LEWK and SAMP stations have the same pattern, namely east-south on the 30-second solution, then changing towards north-east on the daily solution. At the BSIM station, it has almost the same direction towards the northeast, only in the high-rate solution, the north direction is more dominant than the daily solution. In the vertical component, it can be seen that most of them move downwards. This is consistent with the research of Pratama et al. (2018), except for BSIM stations on 30-second solutions. From Figure 3.2, it can be seen that the two solutions have a significant difference in value. This is

supported by the results of the statistical test in Figure 4, where the two solutions are statistically significant at SAMP and LEWK stations.

From Figure 5b, the value and direction of the displacement of the two solutions look similar and not much different. Both solutions are equally directed to the northeast, while the displacement toward the north being more dominant. The two solutions are slightly different; namely, the daily solution is more eastward than the 30-second solution. Statistically, the two points also do not have a significantly different values as was evidence by the rejection of Ho, which means that the two solutions have a displacement value that is not significantly different.

The other two earthquakes, namely Kampungbaru (Mw 6.5) and Simpang (Mw 4.9), are shown in Figure 5c and Figure 5d. These two earthquakes have results similar to the Lombok earthquake. Between the two solutions, there is no significant difference because of the large standard deviation value compared to the value of the difference in displacement. From the earthquake cases used, it can be seen that only large earthquake cases above Mw 6.9 have significantly different results, but this needs to be confirmed again with other earthquake data.

(a)　　　　　　　　　　　　　　　　　　(b)

(c)　　　　　　　　　　　　　　　　　　(d)
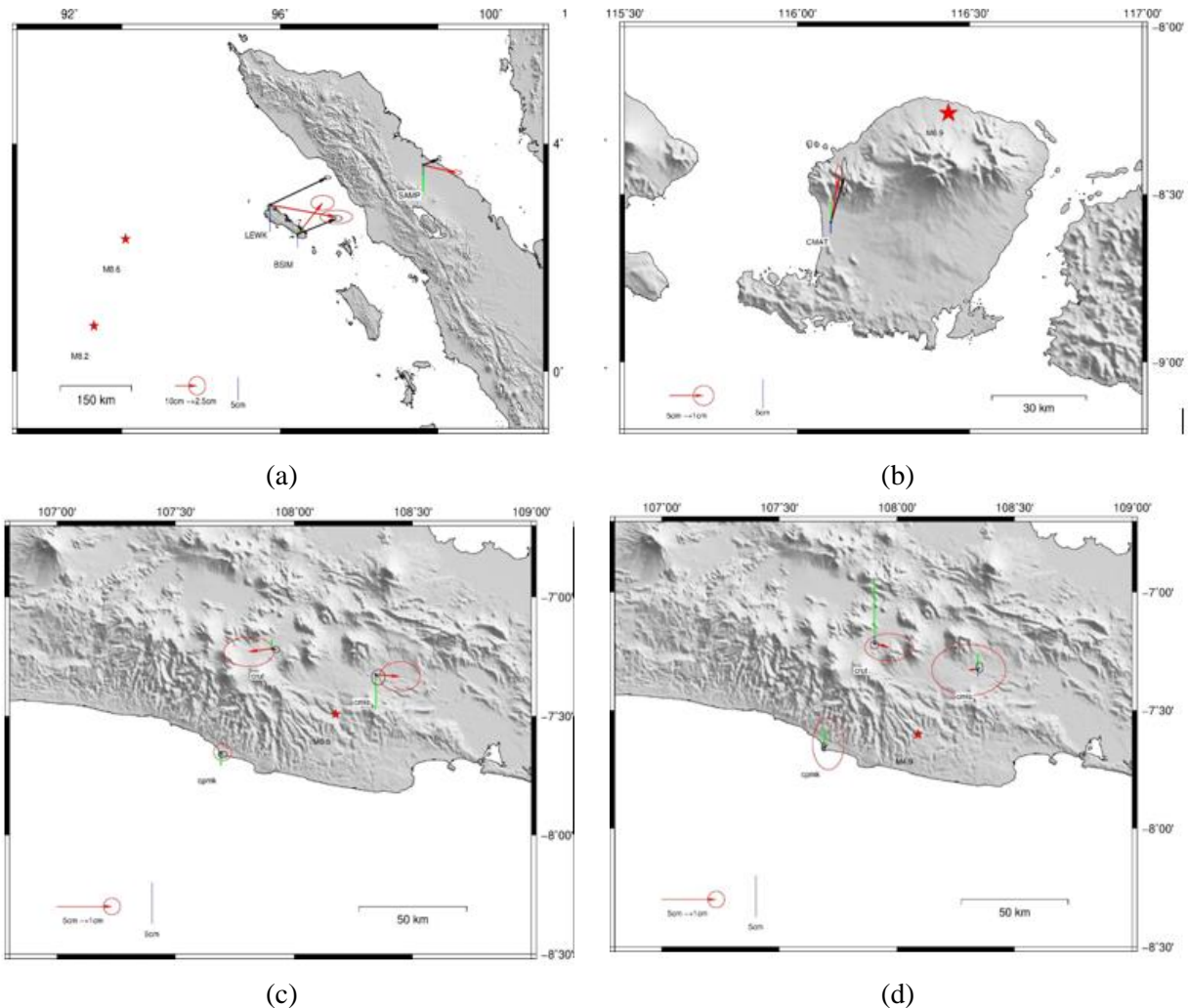
Figure 5. GNSS station displacements for one-minute time span data of 30-second kinematic solution red (Hz) and green (vertical). For daily solutions black (Hz) and blue (vertical) Indian Ocean earthquake Mw 8.6 and 8.2 (a), Lombok Mw 6.9 (b), Kampungbaru Mw 6.5 (c), and Simpang Mw 4.9 (d)

From the explanation above, it can be concluded that the two solutions are significantly different only in the case of the 2012 Indian Ocean great earthquake, while for the other three earthquakes, there is no significant difference. This is possible because the Indian Ocean earthquake rupture duration is relatively long, namely 200 and 60 seconds. Thus it is possible that the GNSS can record well at 30-second intervals. On the other hand, the duration of the rupture is relatively short on the other earthquakes. Therefore for the future, it is hoped that GNSS data be available with a sampling rate higher than the 30-second that is currently available.

4. Conclusion
The processed 30-second interval kinematic

positions with GAMIT Track Kinematic. We can conclude that the information on earthquake coseismic displacements can be obtained by differentiating positions after and before the earthquake rupture. The value of the coseismic displacement of each earthquake is as follows with an accuracy of centimeters (cm). In the case of the Indian Ocean earthquakes (Mw 8.6 and Mw 8.2), the estimated value of the displacement is significantly different for two of the three stations in the 30-second solution as compared with the daily solution. This is possible because apart from the large magnitude, it is also supported by the relatively long duration of the Indian Ocean earthquake rupture; therefore, the 30-second data can record well enough at the time of the earthquake rupture. In this earthquake, the

coseismic displacement value in the 30-second solution is much larger than the daily solution. This indicate that in the cases of these earthquake, the 30-second solution can record information that cannot be recorded by the daily solution.

References
Blaser, L., Krüger, F., Ohrnberger, M., & Scherbaum, F. (2010). Scaling relations of earthquake source parameter estimates with special focus on subduction environment. *Bulletin of the Seismological Society of America*, 100(6), 2914–2926. https://doi.org/10.1785/0120100111.

Chounet, A., Vallée, M., Causse, M., & Courboulex, F. (2018). Global catalog of earthquake rupture velocities shows anticorrelation between stress drop and rupture velocity. *In Tectonophysics,* 733, 148–158. https://doi.org/10.1016/j.tecto.2017.11.005.

Feng, L., Hill, E.M., Banerjee, P., Hermawan, I., Tsang, L.L.H., Natawidjaja, D.H., Suwargadi, B.W., & Sieh, K. (2015). A unified GPS-based earthquake catalog for the Sumatran plate boundary between 2002 and 2013. *In Journal of Geophysical Research B: Solid Earth,* 120 (5), 3566–3598. https://doi.org/10.1002/2014JB011661.

Herring, T., King, R., & McClusky, S. (2015). *GAMIT/GLOBK Reference Manuals, Release 10.6*.

Huang, Y., Yang, S., Qiao, X., Lin, M., Zhao, B., & Tan, K. (2017). Geodesy and Geodynamics Measuring ground deformations caused by 2015 M w7 . 8 Nepal earthquake using high-rate GPS data. *Geodesy and Geodynamics*, 8(4), 285–291. https://doi.org/10.1016/j.geog.2017.03.003.

Kawamoto, S., Ohta, Y., Hiyama, Y., Todoriki, M., Nishimura, T., Furuya, T., Sato, Y., Yahagi, T., & Miyagawa, K. (2017). REGARD: A new GNSS-based real-time finite fault modeling system for GEONET. *Journal of Geophysical Research: Solid Earth*, 122(2), 1324-1349. https://doi.org/10.1002/2016JB013485.

Larson, K.M. (2009). GPS seismology. *Journal of Geodesy*, 83(3–4), 227–233. https://doi.org/10.1007/s00190-008-0233-x.

Pratama, C., Ito, T., Tabei, T., Kimata, F., Gunawan, E., Ohta, Y., Yamashina, T., Nurdin, I., Sugiyanto, D., Muksin, U., Ismail, N., & Meilano, I. (2018). Evaluation of the 2012 Indian Ocean coseismic fault model in 3-D heterogeneous structure based on vertical and horizontal GNSS observation. *AIP Conference Proceedings*, 020011. https://doi.org/10.1063/1.5047296.

Pratama, C., Susanta, F.F., Ilahi, R., Khomaini, A.F., & Abdillah, H.W.K. (2019). Coseismic Displacement Accumulation Between 1996 and 2019 Using A Global Empirical Law on Indonesia Continuously Operating Reference Station (InaCORS). *JGISE: Journal of Geospatial Information Science and Engineering*, 2(2), 237–244. https://doi.org/10.22146/jgise.51130.

Priadi, R., Perdana, Y.H., Wijaya, A., & Suardi, I. (2020). Identification of Source Mechanisms for the August 5 2018 Mw 6.9 and the August 9 2018 Mw7.0 Lombok Earthquakes. *Jurnal Penelitian Fisika Dan Aplikasinya (JPFA)*, 10(1), 44-55. https://doi.org/10.26740/jpfa.v10n1.p44-55.

Pusat Studi Gempa Nasional (2017). *Peta sumber dan bahaya gempa Indonesia tahuan 2017*. Pusat Penelitian dan Pengembangan Perumahan dan Pemukiman Badan Penelitian dan Pengembangan Kementerian Pekerjaan Umum dan Perumahan Rakyat.

Ruhl, C.J., Melgar, D., Grapenthin, R., & Allen, R.M. (2017). The value of real-time GNSS to earthquake early warning. *Geophysical Research Letters*, 44(16), 8311–8319. https://doi.org/10.1002/2017GL074502.

Sarsito, D.A., Andreas, H., Meilano, I., Abidin, H.Z., Darmawan, D., & Gamal, M. (2005). *Implikasi Co-Seismic dan Post-Seismic Horisontal Displacement Gempa Aceh 2004 terhadap Status Geometrik Data Spasial Wilayah Aceh dan Sekitarnya*.

Susilo, Abidin, H.Z., Meilano, I., Sapiie, B., Gunawan, E., Wijarnto, A.B., & Efendi, J. (2017). Preliminary co-sesimic deformation model for Indonesia geospatial reference system 2013. *AIP Conference Proceedings*. https://doi.org/10.1063/1.4987073.

Wei, S., Helmberger, D., & Avouac, J.P. (2013). Modeling the 2012 Wharton basin earthquakes off-Sumatra: Complete lithospheric failure. *Journal of Geophysical Research: Solid Earth*, 118(7), 3592–3609. https://doi.org/10.1002/jgrb.50267.

Wells, D.L., & Coppersmith, K.J. (1994). New empirical relationships among magnitude, rupture length, rupture width, rupture area, and surface displacement. *Bulletin of the Seismological Society of America*, 84(4), 974–1002.

Wessel, P., Smith, W.H.F., Scharroo, R., Luis, J., & Wobbe, F. (2013). Generic Mapping Tools: Improved version released. *EOS Trans. AGU*, 94(45), 409–410. https://doi.org/10.1002/2013EO450001.